CONTRAST MEDIA & MOLECULAR IMAGING

Received: 17 March 2012, Revised: 20 August 2012, Accepted: 15 October 2012, Published online in Wiley Online Library: 2013

(wileyonlinelibrary.com) DOI: 10.1002/cmmi.1517

Spectroscopic, radiochemical, and theoretical studies of the Ga^{3+}-*N*-2-hydroxyethyl piperazine-*N*′-2-ethanesulfonic acid (HEPES buffer) system: evidence for the formation of Ga^{3+}- HEPES complexes in ^{68}Ga labeling reactions

André F. Martins[a,b†], M. I. M. Prata[c,d], S. P. J. Rodrigues[e,f], Carlos F. G. C. Geraldes[a,b,f*], P. J. Riss[g†], A. Amor-Coarasa[h,i], C. Burchardt[h], C. Kroll[h] and F. Roesch[h]

Recent reports have claimed a superior performance of HEPES buffer in comparison to alternative buffer systems for $^{67/68}$Ga labeling in aqueous media. In this paper we report spectroscopic (^{1}H and ^{71}Ga NMR), radiochemical, mass spectrometry and theoretical modeling studies on the Ga^{3+}/HEPES system (HEPES = *N*-2-hydroxyethylpiperazine-*N*′-2-ethanesulfonic acid) performed with the aim of elucidating a potential contribution of HEPES in the $^{68/67}$Ga radiolabeling process. Our results demonstrate that HEPES acts as a weakly but competitive chelator of Ga^{3+} and that this interaction depends on the relative Ga^{3+}: HEPES concentration. A by-product formed in the labeling mixture has been identified as a [^{68}Ga]Ga(HEPES) complex via chromatographic comparison with the nonradioactive analog. The formation of this complex was verified to compete with [^{68}Ga]Ga(NOTA) complexation at low NOTA concentration. Putative chelation of Ga^{3+} by the hydroxyl and adjacent ring nitrogen of HEPES is proposed on the basis of ^{1}H NMR shifts induced by Ga^{3+} and theoretical modeling studies.

Supporting information may be found in the online version of this paper

Keywords: radiolabeling; ^{68}Ga; PET tracers; HEPES buffer–Ga^{3+} interactions; multinuclear NMR; theoretical modeling; mass spectrometry

1. INTRODUCTION

In radiochemistry and radiopharmaceutical chemistry there are numerous examples where the radiolabeling yield and the radiochemical purity of the final solution strongly depend on the pH at which the radiolabeling occurs (1). For this reason the presence of buffers can be very important in this procedure. While many different buffering systems are available, the possibility of forming chelates with buffer agents is an aspect to consider in systems involving trace metals. *N*-2-hydroxyethylpiperazine-*N*′-2-ethanesulfonic acid (HEPES) belongs to a series of buffer compounds introduced by Good and co-workers (2) for use in

* *Correspondence to: Carlos F. G. C Geraldes, Department of Life Sciences, Faculty of Sciences and Technology, University of Coimbra, PO Box 3046, 3001-401 Coimbra, Portugal. E-mail: geraldes@ci.uc.pt*

† *These authors have contributed equally.*

a *A. F. Martins, C. F. G. C. Geraldes*
Department of Life Sciences, Faculty of Sciences and Technology, University of Coimbra, PO Box 3046, 3001-401 Coimbra, Portugal

b *A. F. Martins, C. F. G. C. Geraldes*
Center of Neurosciences and Cell Biology, Largo Marquês de Pombal, University of Coimbra, Portugal

c *M. I. M. Prata*
IBILI, Faculty of Medicine, University of Coimbra, Portugal

d *M. I. M. Prata*
ICNAS, University of Coimbra, Portugal

e *S. P. J. Rodrigues*
Department of Chemistry, Faculty of Sciences and Technology, University of Coimbra, Portugal

f *S. P. J. Rodrigues, C. F. G. C. Geraldes*
Coimbra Chemistry Center, Rua Larga, University of Coimbra, 3004-535 Coimbra, Portugal

g *P. J. Riss*
The Wolfson Brain Imaging Centre, University of Cambridge, Box 65 Addenbrooke's Hospital, Cambridge CB2 0QQ, UK

h *A. Amor-Coarasa, C. Burchardt, C. Kroll, F. Roesch*
Institute of Nuclear Chemistry, Johannes Gutenberg-University, Fritz-Strassmann-Weg 2, 55128 Mainz, Germany

i *A. Amor-Coarasa*
Florida International University, Department of Biomedical Engineering, Miami, Florida, USA

biological studies. HEPES was introduced as an amphoteric that would not form complexes with metal ions in aqueous solution. Although this HEPES property holds quite well for many ions, as confirmed indirectly by numerous studies (2–5), there is a growing evidence of exceptions to this behavior for 2+ metal ions based on kinetics studies (3–5).

The radionuclide ^{68}Ga (β^+, $t_{1/2}$ = 67.7 min) is an important isotope for positron emission tomography (PET), ^{67}Ga (εc, $t_{1/2}$ = 3.35 days) is useful in scintigraphy (6–12). While ^{67}Ga has been very popular in the past, nowadays, generator-derived ^{68}Ga is increasingly used in molecular imaging studies with PET (1,6,7). Besides being generator produced (avoiding the need for an on-site cyclotron), ^{68}Ga has other important advantages, such as a high positron abundance (89%) and its physical half-life, compatible with the pharmacokinetics of most radiopharmaceuticals including small molecules, peptides, aptamers, oligonucleotides and antibody fragments (1,13). The excellent potential of ^{68}Ga-based radiopharmaceuticals in PET diagnosis has been recognized, particularly in oncology (6,7). Although there are several types of these generators, recently TiO_2-based generators have been used in a considerable number of centers worldwide (6,7). This generator provides $^{68}Ga^{3+}$ in 0.1 M HCl.

Among the chelators suitable to complex the Ga^{3+} for *in vivo* use, macrocyclic chelators are very attractive because they display high conformational and size selectivity towards metal ions conferring very high thermodynamic and kinetic stability to their Ga^{3+}chelates (8–12). On the other hand, the formation kinetics of M^{3+}-macrocyclic complexes is very slow and pH-dependent. Under stoichiometric conditions, quantitative conversion of the chelator requires the step-wise addition of base in order to compensate for the release of protons (3 equiv. per mol of Ga^{III}). In contrast, the base can be omitted under no-carrier-added conditions without affecting conversion, owing to the large excess of chelator (1–20 nmol) compared with the radiometal (6 pmol/100 MBq). Under these conditions, however, trace metal contaminants from commercially available reagents easily outweigh the Ga^{3+}, thus imposing considerable competition for the available chelators. In addition, the low concentrations of radiometal solutions (less than 10^{-6} M) has to be considered. For all those reasons, the radiolabeling efficiency of a macrocyclic chelator is largely dependent upon radiolabeling conditions like concentration of the chelator, the presence and concentration of trace metal contaminants, pH, temperature and reaction time.

Complex formation with the pH sensitive Ga^{3+} cation requires mildly acidic conditions to achieve a high radiolabeling yield in a short reaction time (1). This is because the nature of the Ga^{3+} species that are present in aqueous solution, as well as its usefulness in radiochemistry, is determined by the Ga^{3+} hydrolysis processes that strongly depend on the pH (14,15). In aqueous solution, the free hydrated Ga^{3+} ion is stable only under acidic conditions. In the pH range of 3–7 it is prone to hydrolyze, forming gallium trihydroxide, which is insoluble if its free concentration exceeds nanomolar levels. Nevertheless, this can be avoided in the presence of stabilizing agents like HEPES, or other buffers, by maintaining the labeling media within the appropriate range of pH 2.8–3.8. We surmised that some buffers might possibly act as weak chelators that prevent the formation of colloidal gallium before the radiosynthesis of the radiopharmaceutical. HEPES was used as a buffer in a number of studies because it was believed to impose a low risk of complex formation with the radiometal (16–18).

The effect of radiolabeling conditions on radiochemical yields has been the subject of several studies (19–25). Some publications pointed out better performance of $^{67/68}Ga^{3+}$ labeling in HEPES when compared with labeling in alternative buffers (19–24), while one study claimed the equivalence of HEPES, acetate and succinate buffers (25). Velikyan *et al.* followed the time course of the $^{68}Ga^{3+}$ complexation reaction with NOTA ($NOTAH_3$ = 1,4,7-triazacyclononane-1,4,7-triacetic acid) at room temperature for various buffers and found out that high radiochemical yield (>95%) for ^{68}Ga-NOTA was achieved within less than 10 min at room temperature and pH 3.5 using HEPES buffer. In contrast, <80% were found after 10 min using acetate buffer at pH 5.5 (23). In addition, the influence of the buffer seems more pronounced when the concentration of the ligand decreases. A preliminary explanation was that commercial HEPES buffer contains fewer metal impurities than other media currently used and that these impurities strongly influence the radiolabeling. As the coordination chemistry of Ga^{3+} is very similar to that of the Fe^{3+} ion, any Fe^{3+} that is present in the labeling solution, even in very low concentrations, can compromise the radiolabeling yield of the desired product. Another proposed explanation concerned the ability of buffers like acetate to compete with the desired ligands for the metal complexation, especially when buffers are used at high concentrations (24). For example, sodium is weakly complexed by NOTA and acetate forms very weak complexes with Ga^{3+} (26), which does not seem to explain the experimental evidence. However, considering that 100 MBq of ^{68}Ga represent only $6{\cdot}10^{11}$ Ga^{3+} ions whereas 1 M sodium acetate buffer corresponds to 6.10^{20} sodium acetate molecules per millilitre well illustrates the disadvantageous stoichiometry. Under these conditions, the large excess of buffer will doubtlessly influence the complex formation equilibrium, thus competing with ^{68}Ga for the available NOTA chelator.

Hence, a very low interaction between the constituents of the buffer solution and Ga^{3+} cations is desirable. There have been contradictory reports on such interactions between Ga^{3+} and HEPES in aqueous solution. An early report explicitly mentions that no significant interactions between Ga^{3+} and HEPES were found in aqueous solution using ^{71}Ga and ^{1}H NMR (27). However, a recent potentiometric study of the complexation of Ga^{3+} with dipeptides and tripeptides in the presence of biologically relevant zwitterionic buffers reports a formation constant for a 1:1 Ga^{3+}–HEPES species of log $K_1 = 1.99 \pm 0.01$ mol dm^{-3} at 25 °C in the presence of 0.01 mm dm^{-3} KNO_3 (28).

In this paper we report new ^{71}Ga and ^{1}H NMR studies on the interaction of Ga^{3+} and HEPES in solution, in order to elucidate the possible role of the HEPES buffer in the $^{68/67}$Ga radio-labeling as a stabilizing agent. Direct radiochemical evidence on the formation of such a complex and its thin-layer chromatographic (TLC) separation from ^{68}Ga complexes with NOTA and citrate validates the significance of our findings under no-carrier-added conditions. To have further insight into the structures and the stability of Ga^{3+} complexes with HEPES we finally made some theoretical calculations on this system.

2. RESULTS AND DISCUSSION

2.1. NMR studies

2.1.1. ^{71}Ga NMR of the Ga^{3+}–HEPES system

Of the two Ga-isotopes with the same spin quantum number (I = 3/2) that are detectable by NMR, ^{69}Ga and ^{71}Ga, the latter was selected for the NMR study rather than the more abundant ^{69}Ga, owing to its higher sensitivity and lower quadrupole

moment (29). This nucleus differs from the proton in possessing a nuclear quadrupole moment, which results in its relaxation processes being dominated by nuclear quadrupole relaxation, giving rise to very broad NMR signals, especially in an asymmetrical environment (30). This property allows the assessment of the symmetry of Ga^{3+} chelates in solution by analyzing the line-width of the ^{71}Ga NMR signals obtained.

In aqueous solution the pH determines the different kinds of species for the Ga(III) ion, such as $[Ga(H_2O)_6]^{3+}$, $[Ga(OH)(H_2O)_5]^{2+}$, $[Ga(OH)_2(H_2O)_4]^{+}$, $Ga(OH)_3$ and $[Ga(OH)_4]^{-}$ (14). Of these species only those with the most symmetrical environment of the ^{71}Ga nucleus can be observed by NMR, namely $[Ga(H_2O)_6]^{3+}$ (octahedral) and $[Ga(OH)_4]^{-}$ (tetrahedral). In fact, the 0.1 M $Ga(NO_3)_3$ reference solution gave a relatively narrow ^{71}Ga NMR signal ($\Delta\nu_{1/2} = 736 \pm 7$ Hz) at $\delta = 0$ ppm, corresponding to the hydrated cation $Ga(H_2O)_6^{3+}$. (See Fig. S1, Supporting Information.) For the pD range studied (2.0–9.0) a separate ^{71}Ga NMR signal that could be directly assigned to a Ga^{3+}–HEPES stable complex was not observed. At pD 2.0 only a signal corresponding to the hydrated cation $[Ga(H_2O)_6]^{3+}$ is detected in all the formulations. However, its line-width increases substantially with the increase of the [HEPES]/[Ga] ratio in solution, up to $\Delta\nu_{1/2} = 1052 \pm 21$ Hz at at a ratio of 5:1 (Fig. 1), without loss of intensity. This observation was previously attributed to an increase of the viscosity of the solutions (27), but could instead reflect the existence of a weak interaction between HEPES and the cation, for example, through the second-sphere of coordination, or the formation of weak and labile complexes (see theoretical calculations below), which can be responsible for lowering the symmetry of the cation environment, and leading to signal broadening owing to an increased quadrupolar relaxation. Up to pD 3.5 the hexa-aqua ion gives a peak whose intensity gradually falls as the pD value increases. At pD 3.0 (corresponding to pH 2.6), the ^{71}Ga NMR signal broadens dramatically, even in the absence of HEPES ($\Delta\nu_{1/2} = 5000 \pm 100$ Hz), which can be attributed to the presence of different forms of hydrolyzed Ga^{3+} in solution at this pD, in accordance with the literature (14). However, the ^{71}Ga NMR signal line-width increases with the HEPES concentration, up to a value of $\Delta\nu_{1/2} = 9500 \pm 190$ Hz at a 5:1 ratio. The much larger percentage increase in line-width of the Ga^{3+} species in the presence of HEPES at pD 3.0 relative to pD 2.0 is clear evidence of a weak interaction between the hydrated Ga^{3+} species and HEPES (Fig. 1). The reported pK_a values of HEPES (2.99 and 7.42) (31), indicate that a change of pD from 2.0 (pH 1.6) to 3.0 (pH 2.6) leads to a substantial decrease of the degree of ligand protonation, from H_2L^{+}, with both nitrogen atoms protonated, to the presence of almost 50% of the mono-protonated neutral form HL, with the nitrogen atoms less protonated (see later), which promotes the weak interaction with the positively charged Ga(III) species present in solution.

In the pD range 4.0–8.5 (pH 3.6–8.1), the broadening of the ^{71}Ga NMR signal of the Ga^{3+} hydrolyzed species in the absence and presence of HEPES was too extensive to allow the detection of any signal and a white precipitate appears, corresponding to the presence of insoluble $Ga(OH)_3$. At pD 9 and above, the solution becomes clear, as Ga(III) only exists in solution as the $[Ga(OH)_4]^{-}$ species, as shown by its speciation diagram (14). At pD 9, this symmetrical tetrahedral species originated a sharp ^{71}Ga NMR at 170 ppm with a line-width that increases from 136 ± 3 to 186 ± 4 Hz when the [HEPES]/[Ga] ratio rises from 0:1 to 5:1. The very small line-width increase of this species probably results exclusively from the increase of solution viscosity owing to the presence of HEPES.

2.1.2. *^{1}H NMR of the Ga^{3+}–HEPES system*

The microscopic sequence of protonation of the HEPES ligand was investigated by proton NMR pH titrations. The titration curves obtained (Fig. 2) from the spectra (Fig. 3, top) show the chemical shifts of the ligand methylene protons as a function of pD. The protonation of the ligand donor atoms generally results in a de-shielding of its nonlabile hydrogen atoms and changes in chemical shifts can indicate the microscopic sites of protonation at a given solution pH, and thus the ligand protonation sequence (32,33).

Scheme 1 represents the HEPES proton numbering scheme and the protonation sites. The H3 and H4 CH_2 signals are considerably broad, while the others are sharp, owing to the time scale of the internal dynamics of the piperazine ring. The two inflection points of the titration curves define two p*K*a values for HEPES in accordance with the literature (31). The observed

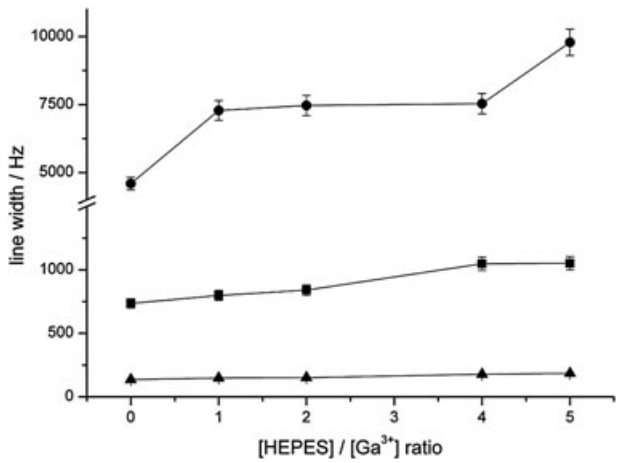

Figure 1. Dependence of the ^{71}Ga NMR signal line width on the [HEPES] / [Ga^{3+}] ratio at different pD values. For pD = 2.0 (■) and 3.0 (●), these data refer to the Ga^{3+} aqueous ion, and for pD = 9.0 (▲) the observed signal corresponds to the $[Ga(OH)_4]^{-}$ species.

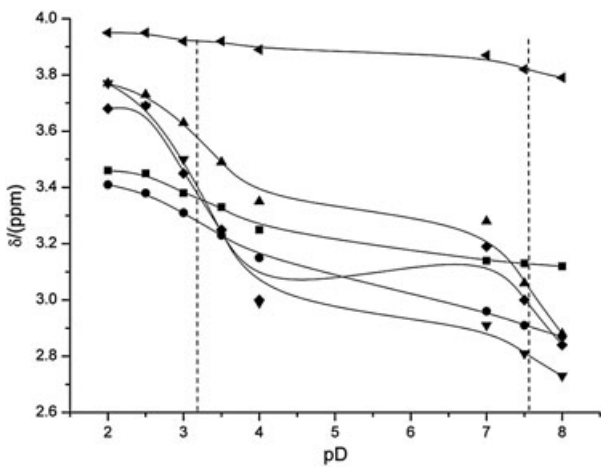

Figure 2. pD dependence of the proton chemical shifts, δ (ppm), for the HEPES ligand. Protons from carbon positions 1 (■), 2 (●), 3 (▲), 4 (▼), 5 (♦), 6 (◄).

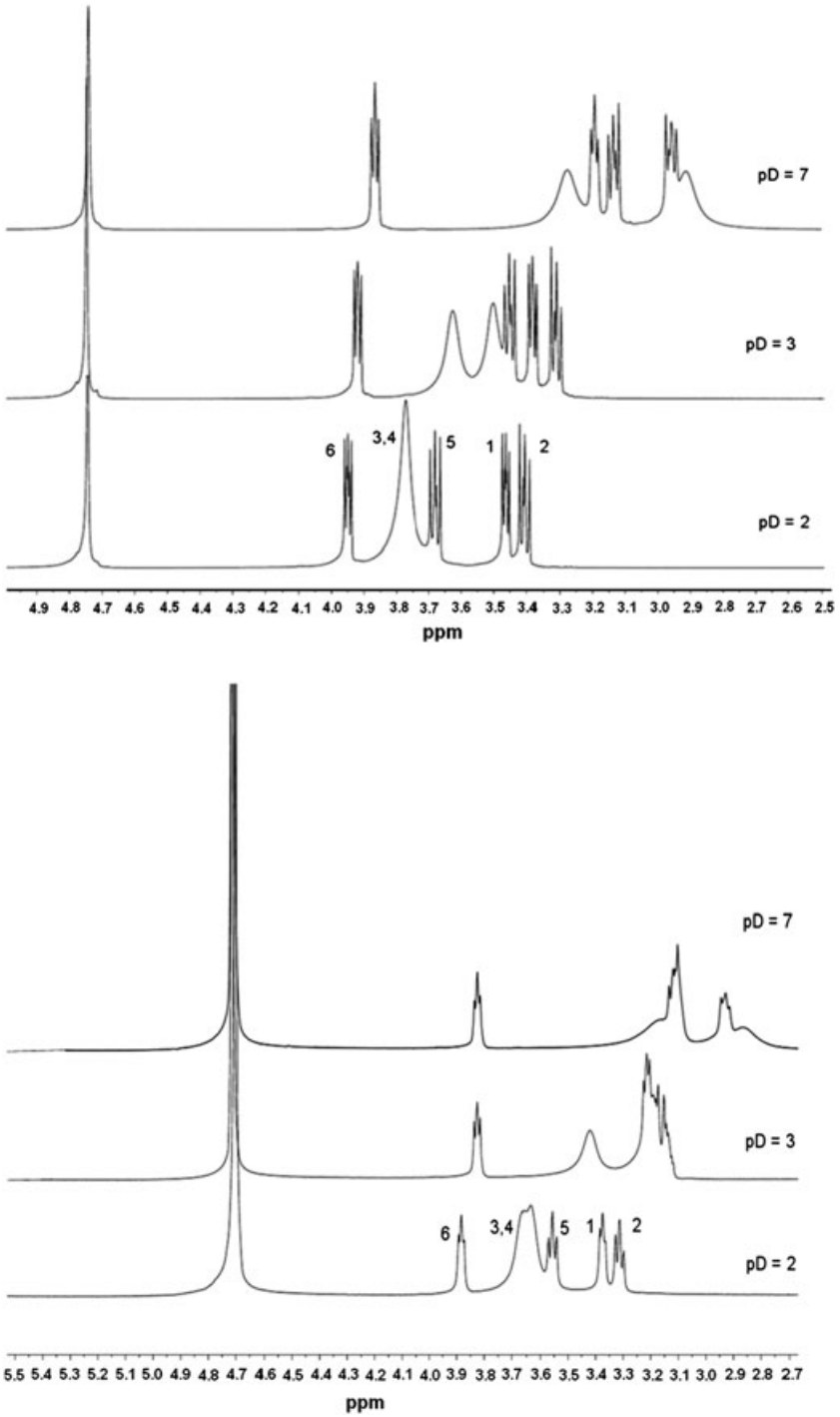

Figure 3. ^{1}H NMR spectra of a 0.5 M HEPES aqueous solution (above) and of a Ga^{3+}–HEPES (M:L, 1:5) solution containing 0.1 M Ga^{3+} (below) at different pD values and 25 °C.

protonation shifts indicate that there is a slight favoring of N1 as the first protonation site. In fact, at the first protonation, the protonation shift of H3 is larger than of H4 CH_2 groups, while at the second protonation the shift of H4 and H5 shifts are larger than for H3 and H2. This is confirmed by our theoretical calculations (see below), which predict that the isomer with N1 protonation is more stable in agreement with X-ray data (34).

Figure 3 also shows proton NMR spectra of aqueous mixtures of HEPES and Ga^{3+} in a 5:1 ratio and of the free ligand at pD 2.0,

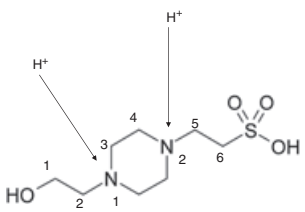

Scheme 1. Structure of HEPES, numbering scheme used for the NMR assignment and nitrogen atom protonation sites.

3.0 and 7.0. At the two first pD values the solutions had no precipitation and were stable, while at pD 7.0 there was some precipitation. However, this solution was analyzed because at this pD (pH 6.6) only the first protonation of HEPES has occurred (species HL present). The interaction of the Ga^{3+} with the ligand barely affects the HEPES signals at pD 2.0, but at pD 3.0 all resonances except H6 (CH_2S protons) are shifted, in particular the H3 and H4 ring protons. Those shifts are almost nonexistent again at pD 7.0, owing to the precipitation of $Ga(OH)_3$. Thus, these data support the existence of a Ga^{3+}–HEPES weak coordination not involving the CH_2S group. These findings are in accordance with modeling studies (see later), which predict the existence of weak stable Ga^{3+}–HEPES complexes with free sulfonate groups.

2.2. Radiochemical studies

The effect of precursor concentration on the radiochemical yield for the formation of NOTA complexes of $^{68}Ga^{3+}$ was examined in water or HEPES buffer at various concentrations. Standard labeling conditions using 400 µl of generator eluate preprocessed by cation exchange chromatography from 50 mCi (1.85 GBq) were used (35,36). The reaction temperature was varied from 45 to 75 °C and the pH was 2.0 (pure water), 2.22 (0.01 M HEPES) and 3.8 (0.1 M HEPES buffer) at 25 °C. Initial labeling experiments were conducted at a 13 nM concentration of NOTA in 0.1 mM HEPES. The NOTA concentration was then reduced in order to investigate the potential of minimizing the precursor concentration for successful ^{68}Ga labeling. As soon as the NOTA concentration was reduced to 3.3 nM, the overall yield of [^{68}Ga]Ga(NOTA) was diminished and formation of an additional ^{68}Ga species was observed. This effect was further pronounced in the lower temperature range around 45 °C and *a fortiori* at a concentration of 0.66 nM (Fig. 4). This product was not observed when the labeling was conducted in H_2O only, that is, without any buffer, at pH 2. [Labeling yields >80% of ^{68}Ga(NOTA) were obtained within 3 min at 60 °C.]

In the analytical studies using TLC, a solution of citrate buffer at pH 4 was used as mobile phase and compared with a citrate free medium (5% sodium chloride–ethanol solution). Using citrate buffer, the yield for this additional radioactive product (identified at R_f value of 0.17) was lower as well, but instead the characteristic [^{68}Ga]Ga(citrate) was formed.

This led us to investigate the formation of this product as a function of the HEPES buffer concentration in the presence and absence of NOTA. First of all, an inverse correlation of the formation of this unknown by-product was found with decreasing NOTA concentration, effectively ruling out NOTA as a source of the by-product. When the HEPES buffer concentration was reduced to 10 mM, the yield of the by-product was lower. No by-product formation was observed using de-ionized water filtered through a 0.54 µm filter membrane (Millipore®) only as reaction solvent. These findings suggest that a weak complex between HEPES and [^{68}Ga]Ga^{3+} is formed whenever a large excess of HEPES over NOTA or sufficient amounts of HEPES in NOTA-free systems is present in the labeling solution.

To scrutinize the possible formation of a ^{68}Ga complex with HEPES, aliquots of the processed generator eluate were heated to 60 °C in purified water at pH 2, 10 and 100 mM HEPES buffer (pH 2.2 and 3.8, respectively), without the addition of NOTA. No ^{68}Ga complex was formed in water, whereas HEPES solutions showed a radioactive product at the same R_f value of 0.17 on the radio-TLC (Figs 4 and 5), indirectly proving the by-product originated from HEPES.

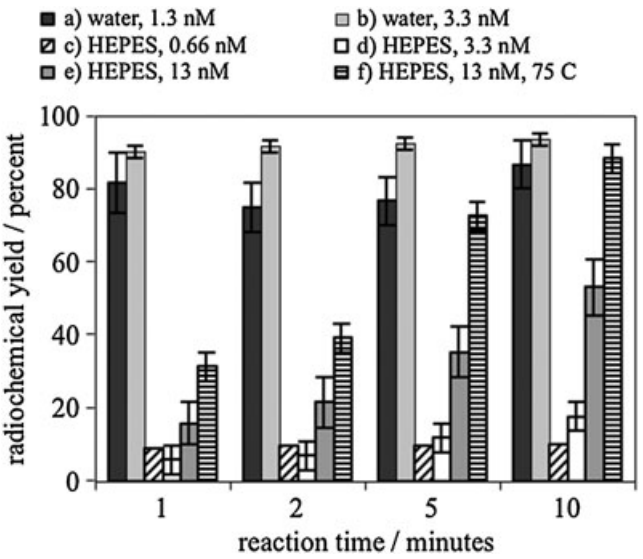

Figure 4. Radiochemical yields for the [^{68}Ga]Ga(NOTA) complex at various chelator concentrations as a function of reaction time at 60 °C in water and 100 mM HEPES buffer and at 75 °C in HEPES buffer: (a) 1.3 nM NOTA in water; (b) 3.3 nM NOTA in water; (c) 0.66 nM NOTA in 100 mM HEPES at pH 3.8; (d) 3.3 nM NOTA in 100 mM HEPES; (e) 13 nM NOTA in 100 mM HEPES; (f) 13 nM NOTA in 100 mM HEPES, 75 °C. Errors are 1 SD.

Using citrate buffer for TLC, free or weakly complexed $^{68}Ga^{3+}$ forms a mixture of ^{68}Ga(citrate)$_n$ species, which result in a characteristic radioactivity distribution from $R_f = 0.3$ to $R_f = 0.8$. In contrast, one single product is observed using NaCl/EtOH solution as mobile phase. In this case, noncomplexed ^{68}Ga species remain at the start, whereas the weakly complexed ^{68}Ga–HEPES species runs to $R_f = 0.1$. Comparable yields were found for both analytical methods (Fig. 6). A control experiment was conducted in HEPES buffer in absence of NOTA, and in this case the putative ^{68}Ga–HEPES complex was formed in high yield (Fig. 6).

To verify the identity of the unidentified product, the formation of crystalline complex was investigated. Although various conditions were examined, only amorphous products were obtained. However, analysis of a concentrated stoichiometric mixture of $GaCl_3$ and HEPES in water by mass spectrometry revealed the presence of a species corresponding to the molar mass of ^{69,71}Ga(HEPES). In addition to this product, the Ga(HEPES)$_2$ complex and several degradation products were found. The obtained product mixture showed a retention factor in the same range as the putative complex formed during the labeling studies on TLC.

In summary, a semi stable ^{68}Ga(HEPES) complex was observed in ^{68}Ga-radiolabeling experiments at low NOTA concentration and moderate temperatures. Theoretical computation and NMR experiments provide insights into the structure, composition and stability of the proposed complex. As the thermodynamic stability constant for Ga(NOTA) complex formation is very high (1,37), and the complex formation is relatively slow, the presence of this complex is probably due to kinetic and stoichiometric reasons. This hypothesis is supported by two key observations: (1) the competitive formation of the HEPES complex can be avoided at higher temperatures as well as (2) by increasing the concentration of NOTA or by reducing the HEPES concentration. These findings suggest that using HEPES buffer may limit the

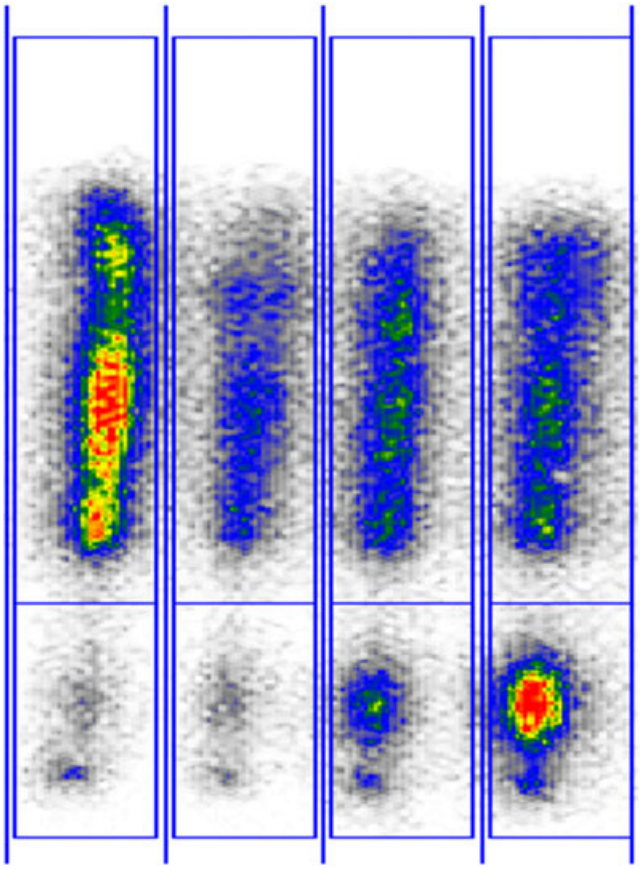

Figure 5. Radio TLC plate (silica gel 60, citrate buffer pH 4) showing the formation of [^{68}Ga]Ga(HEPES) and [^{68}Ga]Ga(citrate) after 1, 2, 5 and 10 min (strips from left to right).

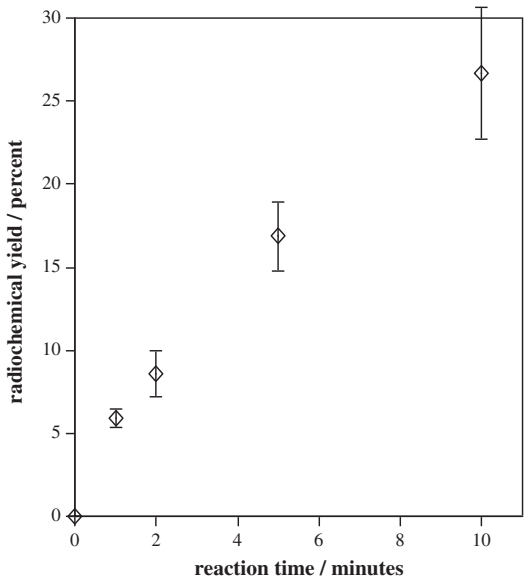

Figure 6. Radiochemical yield of [^{68}Ga]Ga(HEPES) in NOTA-free solutions of HEPES (100 mM, pH 3.8) as a function of reaction time. Errors are 1 SD.

achievable labeling yield when small amounts of the intended ligands such as NOTA or NOTA-conjugated molecular targeting vectors such as, for example, NOTA-octreotides are used. Thereby, HEPES may also exhibit a negative effect on the specific activity of the ^{68}Ga formulation.

2.3. Theoretical studies

The relevant forms of HEPES (denoted L^- and HL, the latter in zwitterionic and neutral forms, with L^- the nonprotonated form), the hexaaquo complex $[Ga(H_2O)_6]^{3+}$ and $[GaL(H_2O)_n]^{2+}$ ($n = 3, 4$) complexes, in their various possible protonation forms, have been studied with solvation (C-PCM) corrections for water solvent. One must note that, for the present systems, solvation corrections are indeed fundamental to obtain meaningful results. In fact, the zwitterionic forms of HL only become more stable than the neutral form when a solvation model is employed. Moreover, the stable theoretical structures obtained in vacuum show apparently unphysical interactions between the sulfonate group and the complexing water molecules or even with the gallium ion. The need of solvation corrections for modeling metal ion complexes in solution is well known and justified (38).

The electronic energy (in the solvent) of the chemical species studied was minimized starting with structures taken from experimental results for similar complexes (2) and X-ray data (34). The Hessians were computed to confirm that the obtained structures were energy minima, to obtain their thermodynamic properties and to estimate thermal energies. For the most relevant chemical species obtained at the C-As an anionic species (L^-) and bare amine nitrogens are involved, the use of diffuse basis sets is fundamental to obtain reasonable energies, but the geometries obtained at the lower level 6-31 G(d,p)/B3LYP for some of the complexes (not presented in this work) are not significantly different. As far as we know, from the set of chemical species studied in this work, only the hexaaquogallium (III) ion $[Ga(H_2O)_6]^{3+}$ has been studied by theoretical methods (39,40). Our results for geometries and symmetry of the complex are in agreement with the results that have been obtained without solvation corrections, but employing a second sphere of coordination.

Figure 7 shows two perspective views of the $[GaL(H_2O)_4]^{2+}$ complex obtained from our DFT calculations (hydrogens are not shown for simplicity). As can be seen, the chemical environment around Ga^{3+} (with coordination number six) is highly asymmetric. In Table 1, some structural parameters are presented. The Ga–O_w distances for the complex are somehow longer, but of the same order of magnitude as those of the $[Ga(H_2O)_6]^{3+}$ complex. The protonated form $[GaHL(H_2O)_4]^{3+}$ has been also studied. Although being a true minimum in the potential energy surface, its energy is too high to be a relevant species, which is in agreement with results for Cu^{2+} (2). The zwitterionic form of $[GaL(H_2O)_3]^{2+}$, with the free nitrogen protonated and an hydroxyl anion attached to gallium ion, $[GaHL(OH)(H_2O)_3]^{2+}$, shows the highest stability. The other isomeric zwitterionic structures with the same total charge have not been studied, but similar stabilities are expected.

The relative stability of the complexes in aqueous solution against hydroxide attack is a point of interest. Although such estimates are not yet very accurate, mainly owing to errors resulting from the solvation models, we estimated equilibrium constants for the relative stability of the Ga^{3+}–HEPES complexes. The standard thermodynamic cycle involving the gas phase was used but, as zwitterionic species are involved, we have taken the additional approximation of employing the geometries obtained in solvent calculations to estimate gas phase energies and Gibbs contributions from internal degrees of freedom. The usual conversion from 1 atm gas phase reference to 1 M reference in solution, $RT \ln(RT/p)$, as well as corrections owing to the presence of

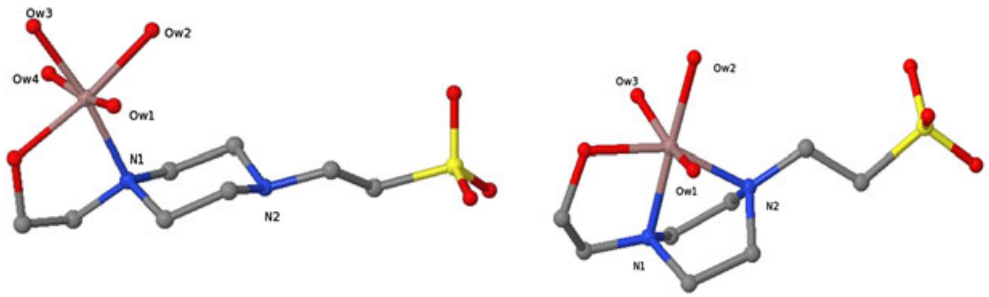

Figure 7. Three-dimensional perspective views of the $GaL(H_2O)_n^{2+}$ (L = HEPES, $n = 3$, 4) complexes. Hydrogen atoms are not shown for clarity. The nitrogen positions (N) and water oxygen (Ow) coordination sites are indicated.

Table 1. Structural properties of selected complexes obtained at 6-31++G(d,p)/B3LYP level with C-PCM model using GAMESS code.

Chemical species	Bond	Distance (Å)
$[GaL(H_2O)_4]^{2+}$	Ga-N1	2.09
	Ga-O_{OH}	1.99
	Ga-O_{w1}	2.03
	Ga-O_{w2}	2.01
	Ga-O_{w3}	2.03
	Ga-O_{w4}	2.04
$[GaL(H_2O)_3]^{2+}$	Ga-N1	2.05
	Ga-N2	2.1
	Ga-O_{OH}	2.03
	Ga-O_{w1}	2.09
	Ga-O_{w2}	1.99
	Ga-O_{w3}	2.07
$[Ga(H_2O)_6]^{3+}$	Ga-O_w	1.98

water as reactant or product (41), $RT \ln[H_2O]$, are used. The calculated equilibrium constants for the processes

$$[Ga(H_2O)_6]^{3+}(aq) + L^-(aq) \leftrightarrow [GaL(H_2O)_n]^{2+}(aq) + (6-n)\,H_2O\,(l) \quad (1)$$

are 2×10^8 and 81 for $n = 3$ and 4, respectively. The first of these values is probably too high, while the second is probably too low, although the latter is in agreement within one order of magnitude with the experimental reported value of $\log K = 1.99 \pm 0.01$ (28). For the zwitterionic species $[GaHL(OH)(H_2O)_3]^{2+}$, the value 2×10^{20} is obtained. The first type of complex ($n = 3$), where Ga^{3+} interacts with both nitrogen atoms, although compatible with our ^{1}H NMR data, is not observed for Cu^{2+} complexes (2). This is in agreement with the kinetics controlled mechanism proposed for the formation of these complexes (2): favored by the OH group and disfavored owing to the presence of the bulky sulfonate group.

From Table 2 we can also estimate the relative stability of the zwitterionic and neutral forms of HEPES. The zwitterionic form with H@N1 is favored by $\Delta G = 9.5$ kJ mol^{-1} giving an equilibrium constant of 46. This zwitterionic form with H@N1 is also more stable than the neutral form by $\Delta G = 46.0$ kJ mol^{-1}.

Our results are compatible with the HEPES interaction with Ga^{3+} at low pH values. In fact, owing to the equilibrium HL ↔ $L^- + H^+$ ($pK_a = 7.42$), the ratio of concentrations $[[GaL(H_2O)_n]^{2+}(aq)]/[[Ga(H_2O)_6]^{3+}(aq)]$, although decreasing with pH, but increasing with HL concentration, will not be negligible for pH > 3.

Table 2. Gibbs energies calculated at the 6-31++G(d,p)/B3LYP level with C-PCM model using GAMESS code

Chemical species	E(ele, sol)/E_h	G(int) (kJmol$^{-1)}$
$GaL(H_2O)_4^{2+}$	−3353.042939	897.1
$GaHL(OH)(H_2O)_3^{2+}$	−3353.085871	906.6
$GaHL(H_2O)_4^{2+}$	−3353,466546	960,5
$GaL(H_2O)_3^{2+}$	−3276,635857	834.0
$Ga(H_2O)_6^{3+}$	−2382.506940	359.5
L^-	−1123.349329	592.5
HL (zwitterion, H@N1)	−1123.803694	640.8
HL (zwitterion, H@N2)	−1123.802362	646.7
HL (neutral)	−1123.779511	624.2
H_2O	−76.406331	7.3

In summary, the results obtained by NMR spectroscopy in aqueous solution are supported by the modeling studies in what concerns the Ga^{3+}–HEPES interference at the pH conditions usually employed for radiolabeling.

3. CONCLUSIONS

It has been reported by various methods that the HEPES buffer interacts weakly with some cations in solution, such as Pb^{2+} (42) and Cu^{2+} (2,31,43) in solution, but not with Zn^{2+} or Cd^{2+} (39,40). The interaction with Cu^{2+} has been well characterized, and was proposed to involve a weak interaction of Cu^{2+} with the hydroxyl oxygen of HEPES, followed by transient chelate formation involving also binding of the adjacent ring nitrogen (N1, see Scheme 1). The present work describes spectroscopic (^{1}H and ^{71}Ga NMR), mass spectrometry and radiochemical data, also supported by theoretical modeling studies on the Ga^{3+}–HEPES system. We conclude that HEPES buffer used in the $^{68/67}$Ga radiolabeling process is an undeniable, but weakly competitive chelator of Ga^{3+} that interferes with the radiolabeling process. Our findings are in accordance with potentiometric studies, which proposed formation of a very weak 1:1 complex in solution (28). The formed complex was identified as a [^{68}Ga]Ga(HEPES) species via chromatographic comparison with the nonradioactive analog. Formation of a weak Ga(HEPES) complex is competing with Ga(NOTA) complex formation, presumably owing to the large excess of HEPES, which compensates for the larger kinetic stability of the NOTA complex. This effect may occur too in the case of other macrocyclic or nonmacrocyclic ligands. The ^{1}H NMR shifts induced by Ga^{3+} and the theoretical studies rationalize the data, pointing to preferential chelation of Ga^{3+} by the hydroxyl and adjacent ring nitrogen of HEPES.

4. MATERIALS AND METHODS

4.1. Materials

The triaza macrocyclic ligand NOTA was synthetized according to a published procedure (44). All other chemicals used in this work were obtained from commercial suppliers as specified. HEPES buffer sodium salt was obtained in its highest purity (>99.5%) and used without further purification.

4.2. NMR studies

D_2O solutions containing 0.1 M Ga^{3+} and HEPES in different stoichiometric ratios (Ga^{3+}–HEPES 1:1, 1:2, 1:4, 1:5) were prepared. The pD of the solutions was adjusted with CO_2-free NaOD and DCl and measured with a Crison MicropH 2002 pH meter, equipped with an Ingold 405-M5 combined electrode. The isotopic correction pD = pH + 0.4 (45) was not done, so the directly measured pD values have been used.

^{1}H and ^{71}Ga NMR spectral measurements were performed with an 11.744 T magnet Varian Unity 500 spectrometer operating at 499.843 and 152.426 MHz, respectively. The ^{1}H resonance shifts were measured relative to sodium 3-trimethylsilyl-9-propanesulfonate and the ^{71}Ga chemical shifts were measured relative to the $Ga(H_2O)_6^{3+}$ species present in a 0.1 M $Ga(NO_3)_3$ solution in D_2O, used as external reference. Assignments of the proton NMR spectra were based on literature data for similar systems and in the results of two-dimensional homonuclear correlation spectra (COSY). NMR spectra were obtained at 25 °C in the pD range of 2.0–7.0.

4.3. Mass spectrometry

Ga-NOTA was dissolved in water (0.1 mg ml^{-1}) for mass spectrometry (Fluka) and analyzed by electron spray ionization mass spectrometry on a Micromass Q-TOF Ultima 3 spectrometer at a resolution of 0.01 *m/z*.

4.4. Radiolabeling procedure

A TiO_2-based $^{68}Ge/^{68}Ga$ radionuclide generator commercially available from Cyclotron Co., Obninsk, Russia, was used. A stock solution of NOTA was prepared with 1 mg of the pure product in 1 ml of Millipore water (1 mg ml^{-1}). This solution was used to prepare the labeling vessels for all the experiments. The experiments were carried out by adding the 400 µl elution from the generator to 5 ml of HEPES buffer (pH = 3.7, Merck KGaA, Germany, or Sigma-Aldrich Chemie GmbH, Germany), 0.5 ml of HEPES buffer in 4.5 ml of water or pure water and preheating the sample for 10 min. Subsequently, a defined volume of NOTA stock solution was added. The volumes used were 1, 5 and 20 µl (1, 5 and 20 µg, respectively) at a temperature of 60 and 75 °C. Samples (1 µl) were taken after 1, 2, 5 and 10 min, placed on a silica gel-coated TLC plate (5 × 10 cm, Merck KGaA, Darmstadt, Germany) and run in two different solvents: 5% aqueous NaCl/EtOH (7:3) and citrate buffer (pH = 4, Merck KGaA, Darmstadt Germany). Detection was performed using a Canberra InstantImager for radioactivity, UV lamp, iodine on silica gel and potassium permanganate solution.

4.5. Formation of a nonradioactive Ga–HEPES solution

HEPES (0.11 mmol, 241 mg) and $GaCl_3$ (0.1 mmol, 17.6 mg) were dissolved in D_2O (1 ml) under sonication. The solvent was removed by evaporation *in vacuo* and the residue was taken up in D_2O (1 ml). The obtained solution was used for mass spectrometry measurements. MS(ESI) *m/z* found: 305.06 (M^+, 9.33%), 307.05 (M^+, 2.23).

4.6. Modeling studies

Electronic structure calculations have been performed using GAMESS suite (version R3, 12 January 2009) (46,47) at the density functional theory (DFT) level with the 6-31++G(d,p) basis set (48–51) using the B3LYP functional (as implemented in GAMESS code). The conductor-like polarizable continuum model (C-PCM) (52–55) with iterative solver, as implemented in GAMESS (56) was also used for water solvent. Internal default parameters were used for water ($\varepsilon = 78.39$, $R_{Sol} = 1.385$ Å). The calculations were for $T = 298.15$ K and only electrostatic contributions were considered for the solvent model. The atomic radii used in the C-PCM calculation for defining the cavities were the standard van der Waals values implemented in the code (for gallium the value of 1.87 Å was considered).

5. Supporting Information

^{71}Ga NMR spectra of D_2O solutions containing 0.1 M Ga^{3+} and HEPES in increasing stoichiometric [HEPES]/[Ga^{3+}] ratios at pD = 2.0, and cartesian coordinates for all optimized structures can be found in the online version of this article.

Acknowledgments

This work was supported by Fundação para a Ciência e Tecnologia, Portugal, under projects PTDC/QUI/70063/2006 and PTDC/QUI-QUI/099744/2008. The F.R. team is grateful to the 'Fonds der Chemischen Industrie' (Germany) for the donation of various chemicals and solvents. The European networks COST D38 and COST TD1004. Actions are gratefully acknowledged. A.A.C. thanks the IAEA for a fellowship under the Agency's Technical Cooperation Programme.

REFERENCES

1. Roesch F, Riss PJ. The Renaissance of the $^{68}Ge/^{68}Ga$ radionuclide generator initiates new developments in ^{68}Ga radiopharmaceutical chemistry. Curr Top Med Chem 2010; 10: 1633–1668.
2. Good NE, Winget GD, Winter W, Connolly TN, Izawa S, Singh RMM. Hydrogen ion buffers for biological research, Biochemistry 1966; 5: 467–477.
3. Turant TS, Rorabacher DB. Steric effects in chelation kinetics. III. Reaction of aquonickel (II) ion with N-alkyl-substituted ethylediamines. Inorg Chem 1971; 11: 288–295.
4. Yu Q, Kandegedara A, Xu Y, Rohrabacher DB. Avoiding interferences from Good's Buffers: a contiguous series of non-complexing tertiary amine buffers covering the entire range of pH 3–11. Anal Biochem 1997; 253: 50–56.
5. Kandegedara A, Rorabacher DB. Non-complexing tertiary amines as 'better' buffers covering the range of pH 3–11. Temperature dependence of their acid dissociation constants. Anal Chem 1999; 71: 3130–3144.
6. Maecke HR, André JP. ^{68}Ga-PET radiopharmacy: a generator-based alternative to ^{18}F-radiopharmacy. PET Chemistry, the Driving Force in Molecular Imaging, Schubiger PA, Lehmann L, Friebe M, editors. Springer: Berlin, 2007.
7. Jurisson S, Berning D, Jia W, Ma D. Coordination compounds in nuclear medicine. Chem Rev 1993; 93: 1137–1156.
8. Sá A, Matias AA, Prata M I M, Geraldes CFGC, Ferreira PMT, André JP. Gallium labeled NOTA-based conjugates for peptide receptor-mediated medical imaging. Bioorg Med Chem Lett 2010; 20: 7345–7348.
9. Fontes A, Prata MIM, Geraldes CFGC, André JP. Ga(III) chelates of amphiphilic DOTA-based ligands: synthetic route and in vitro and in vivo studies. Nucl Med Biol 2011; 38: 363–370.

10. Riss PJ, Burchardt C, Roesch F. A methodical ^{68}Ga-labelling study of DO2A-(butyl- L-tyrosine)$_2$ with cation-exchanger post-processed ^{68}Ga: practical aspects of radiolabelling. Contrast Media Mol Imag 2011; 6: 1555–4317.
11. Riss PJ, Kroll C, Nagel V, Roesch F.. NODAPA-OH and NODAPA-(NCS)$_n$: synthesis, ^{68}Ga-radiolabelling and in vitro characterisation of novel versatile bifunctional chelators for molecular imaging. Bioorg Med Chem Lett 2008; 18: 5364–5367.
12. Burchardt C, Riss PJ, Zoller F, Maschauer S, Prante O, Kuwert T, Roesch F. [^{68}Ga]Ga-DO$_2$A-(OBu-L-tyr)$_2$: synthesis, ^{68}Ga-radiolabeling and in vitro studies of a novel ^{68}Ga-DO$_2$A-tyrosine conjugate as potential tumor tracer for PET. Bioorg Med Chem Lett 2009; 19: 3498–3501.
13. Ginj M, Maecke H. Radiometallo-labeled peptides in tumor diagnosis and therapy. Metal Ions Biol Syst 2004; 42: 109–142.
14. Haues RL, Hubner KF. Basis for the clinical use of gallium and indium radionuclides. Metal Ions Biol Syst 1984; 16: 279–315.
15. Reichert DE, Lewis JS, Anderson CJ. Metal complexes as diagnostic tools. Coord Chem Rev 1999; 184: 3–66.
16. Breeman WAP, de Jong M, de Blois E, Bernard BF, Konijenberg M, Krenning EP. Radiolabelling DOTA-peptides with Ga-68. Eur J Nucl Med Mol Imag 2005; 32: 478–485.
17. Meyer G-J, Mäcke H, Schuhmacher J, Knapp WH, Hofmann M. ^{68}Ga-labelled DOTA-derivatised peptide ligands. Eur J Nucl Med Mol Imag 2004; 31: 1097–1104.
18. Green AM, Welch MJ. Gallium radiopharmaceutical chemistry. Int J Radiat Appl Instrum Part B 1989; 16: 435–448.
19. Eisenwiener K-P, Prata MIM, Zhang H-W, Buschmann I, Santos AC, Reubi J-C, Wenger S, Maecke HR. NODAGATOC, a new [$^{67/68}$Ga] and [^{111}In] peptide for SPECT, PET (and therapeutic applications) of somatostatin receptor (hsst2) expressing tumors. Bioconjug Chem 2002; 13: 530–541.
20. Velikyan I, Maecke H,Langstrom B. Convenient preparation of ^{68}Ga-based PET-radiopharmaceuticals at room temperature. Bioconjug Chem 2008; 19: 569–573.
21. Eder M, Waengler B, Knackmuss S, LeGall F, Little M, Haberkorn U, Mier W, Eisenhut M. Tetrafluorophenolate of HBED-CC: a versatile conjugation agent for ^{68}Ga-labeled small recombinant antibodies. Eur J Nucl Med Mol Imag 2008; 35: 1878–1886.
22. Sasson R, Vaknin D, Bross A, Lavie E. Determination of HEPES in ^{68}Ga-labeled peptide solutions. J Radioanal Nucl Chem. 2010; 283: 753–756.
23. Velikyan I, Beyer GJ, Bergström-Pettermann E, Johansen P, Bergström M, Långström B. The importance of high specific radioactivity in the performance of ^{68}Ga-labeled peptide. Nucl Med Biol 2008; 35: 529–536.
24. Velikyan I, Beyer GJ, Långström B. Microwave-supported preparation of ^{68}Ga bioconjugates with high specific radioactivity. Bioconjug Chem 2004; 15: 554–560.
25. Bauwens M, Chekol R, Vanbilloen H, Bormans G, Verbruggen A. Optimal buffer choice of the radiosynthesis of ^{68}Ga-DOTATOC for clinical application. Nucl Med Commun 2010; 8: 753–758.
26. Clausén M, Öhman L-O, Kubicki JD, Persson P. Characterization of gallium(III)-acetate complexes in aqueous solution: a potentiometric, EXAFS, IR and molecular orbital modelling study. J Chem Soc Dalton Trans 2002; 2559–2564; DOI: 10.1039/B111408E
27. Chang CHF, Pitner TP, Lenkinski RE, Glickson JD. The interaction of gallium with various buffers and chelating agents in aqueous solution: gallium-71 and hydrogen-1 NMR studies. Bioinorg Chem 1978; 8: 11–19.
28. Azab HA, Abou El-Nour KM, Sorror SH. Metal ion complexes containing dipeptides, tripeptides, and biologically important zwitterionic buffers. J Chem Eng Data 2007; 52: 381–390.
29. Akitt JW. Nuclear magnetic resonance spectroscopy in liquids containing compounds of aluminium and gallium. Ann Rep NMR Spectrosc 1972; 5B: 465–556.
30. Prata MIM, Santos AC, Geraldes CFGC, de Lima JJP. Structural and in vivo studies of metal chelates of Ga(III) relevant to biomedical imaging. J Inorg Biochem 2000; 79: 359–363.
31. Sokołowska M, Bal W. Cu(II) complexation by 'non-coordinating' N-2-hydroxyethylpiperazine-N′-2-ethanesulphonic acid (HEPES buffer). J Inorg Biochem 2005; 99: 1653–1660.
32. Sudmeier JL, Relley CN. Nuclear magnetic resonance studies of protonation of polyamine + aminocarboxylate compounds in aqueous solution. Anal Chem 1964; 36: 1698–1706.
33. Geraldes CFGC, Urbano AM, Alpoim MC, Sherry AD, Kuan K-T, Rajagopalan R, Maton F, Muller RN. Preparation, physicochemical characterization, and relaxometry studies of various gadolinium (III)-DTPA-bis(amide) derivatives as potential magnetic-resonance contrast agents. Magn Reson Imag 1995; 13: 401–420.
34. Wouters J, Häming L, Sheldrick G. HEPES. Acta Cryst 1996; C52: 1687–1688.
35. Zhernosekov KP, Filosofov DV, Baum RP, Aschoff P, Bihl H, Razbash AA, Jahn M, Jennewein M, Rösch F. Processing of generator-produced ^{68}Ga for medical application. J Nucl Med 2007; 48: 1741–1748.
36. Asti M, De Pietria G, Fraternalia A, Grassib E, Sghedonib R, Fioronib F, Roesch F, Versaria A, Salvoa D. Validation of ^{68}Ge/^{68}Ga generator processing by chemical purification for routine clinical application of ^{68}Ga-DOTATOC. Nucl Med Biol 2008; 35: 721–724.
37. Martell AE, Motekaitis RJ, Clarke ET, Delgado R, Rong YS. Stability constants of metal complexes of macrocyclic ligands with pendant donor groups. Supramol Chem 1996; 6: 353–363.
38. Hocking RK, Deeth RJ, Hambley TW. DFT study of the systematic variations in metal–ligand bond lengths of coordination complexes: the crucial role of the condensed phase. Inorg Chem 2007; 46: 8238–8244.
39. Rudolph WW, Pye CC. Gallium(III) hydration in aqueous solution of perchlorate, nitrate and sulfate. Raman and 71-Ga NMR spectroscopic studies and ab initio molecular orbital calculations of gallium(III) water clusters. Phys Chem Chem Phys 2002; 4: 4319–4327.
40. Rudolph WW, Pye CC, Irmer G. Study of gallium(III) nitrate hydrate and aqueous solutions: Raman spectroscopy and ab initio molecular orbital calculations of gallium(III) water clusters. J Raman Spectrosc 2002; 33: 177–190.
41. Pliego Jr, JR. Thermodynamic cycles and the calculation of pKa. Chem Phys Lett 2003; 367: 145–149.
42. Soares HMVM, Conde PCFL. Electrochemical investigations of the effect of N-substituted aminosulponic acids with a piperazinic ring pH buffers on heavy metal processes which may have implications on speciation studies. Anal Chim Acta 2000; 421: 103–111.
43. Mash HE, Chin H, Sigg L, Hari R, Xue H. Complexation of copper by zwitterionic aminosulfonc (Good) buffers. Anal Chem 2003; 75: 671–677.
44. Geraldes CFGC, Alpoim MC, Marques MPM, Sherry AD, Singh M. NMR and potentiometric studies of the protonation scheme of a triazatriacetic macrocycle and its complexes with lanthanum and lutetium. Inorg Chem 1985; 24: 3876–3881.
45. Glasoe PK, Long FA. Use of glass electrodes to measure acidities in deuterium oxide. J Phys Chem 1960; 64: 188–189.
46. Schmidt MW, Baldridge KK, Boatz JA, Elbert ST, Gordon MS, Jensen JJ, Koseki S, Matsunaga N, Nguyen KA, Su S, Windus TL, Dupuis M, Montgomery JA Jr. The General Atomic and Molecular Electronic Structure System. J Comp Chem 1993; 14: 1347–1363.
47. Gordon MS, Schmidt MW. Theory and Applications of Computational Chemistry, the first Forty Years, Dykstra CE, Frenking G, Kim KS, 1 GE, editors. Elsevier: Amsterdam, 2005; 1167–1189.
48. Ditchfield R, Hehre WJ, Pople JA, Self-consistent molecular-orbital methods. IX. An extended Gaussian-type basis for molecular-orbital studies of organic molecules. J Chem Phys 1971; 54: 724–728.
49. Hehre WJ, Ditchfield R, Pople JA. Self-consistent molecular orbital methods. XII. Further extensions of Gaussian-type basis sets for use in molecular orbital studies of organic molecules. J Chem Phys 1972; 56: 2257–2261.
50. Hehre WJ, Ditchfield R, Pople JA. Influence of polarization functions on molecular-orbital hydrogenation energies. Theor Chim Acta 1973; 28: 213–222.
51. Rassolov VA, Ratner MA, Pople JA, Redfern PC, Curtiss LA. 6-31 G* basis set for third-row atoms. J Comput Chem 2001; 22: 976–984.
52. Miertus S, Scrocco E, Tomasi J. Electrostatic interaction of a solute with a continuum. A direct utilization of ab initio molecular potentials for the prevision of solvent effects. J Chem Phys 1981; 55: 117–129.
53. Miertus S, Tomasi J. Approximate evaluation of the electrostatic free energy and internal energy changes in solution processes. Chem Phys 1982; 65: 239–245.
54. Cossi M, Barone V, Cammi R, Tomasi J. Ab initio study of solvated molecules: a new implementation of the polarizable continuum model. Chem Phys Lett 1996; 255: 327–335.
55. Tomasi J, Mennucci B, Cammi R. Quantum mechanical continuum solvation models. Chem Rev 2005; 105: 2999–3093.
56. Li H, Jensen JH. Improving the efficiency and convergence of geometry optimization with the polarizable continuum model: new energy gradients and molecular surface tessellation. J Comput Chem. 2004; 25: 1449–1462.

